energies

MDPI

Article

Novel Approach to Diagnose Safe Electrical Power Distribution

Lars Braun [1,*], Minh Le [1], Jürgen Motz [1] and Kai Peter Birke [2]

[1] Robert Bosch GmbH, Mittlerer Pfad 9, 70499 Stuttgart, Germany; minh.le@de.bosch.com (M.L.); juergen.motz@de.bosch.com (J.M.)
[2] Electrical Energy Storage Systems, Institute for Photovoltaics, University of Stuttgart, Pfaffenwaldring 47, 70569 Stuttgart, Germany; peter.birke@ipv.uni-stuttgart.de
* Correspondence: lars.braun2@bosch.com

Abstract: The integrity of the 12 V dc power distribution system on a vehicle is essential to guarantee continuous power supply to safety-relevant consumers. Safety-relevant consumers are critical loads, for example, electric power steering, braking systems with functionalities like Anti-Lock Braking or Electronic Stability Control, and autonomous drive systems. To prevent insufficient power supply for safety-relevant consumers due to an increased wiring harness resistance, a novel diagnostic approach is developed to determine the condition of the power distribution, especially the electrical resistance. The influence of measurement errors and bus commutation on the estimation is investigated by using a simulation. By using the diagnostic, a resistance determination in the milliohm range with a standard deviation of $\sigma = 0.3\,\mathrm{m\Omega}$ can be achieved under realistic conditions. This ensures that failures in the wiring harness can be identified, avoiding cascading effects and minimizing recalls. Compared to the state of the art, redundancies, costs, and weight can be saved with the proposed diagnostic system based on electrical resistance estimation.

Keywords: automotive electronics; diagnostic; electric power steering; safe power distribution; powernet; power supply system; wiring harness

check for updates

Citation: Braun, L.; Le, M.; Motz, J.; Birke, K.P. Novel Approach to Diagnose Safe Electrical Power Distribution. *Energies* **2024**, *17*, 5685. https://doi.org/10.3390/en17225685

Academic Editor: Tapas Mallick

Received: 17 October 2024
Revised: 2 November 2024
Accepted: 5 November 2024
Published: 14 November 2024

Copyright: © 2024 by the authors. Licensee MDPI, Basel, Switzerland. This article is an open access article distributed under the terms and conditions of the Creative Commons Attribution (CC BY) license (https://creativecommons.org/licenses/by/4.0/).

1. Introduction

Failure in the operation of safety-relevant systems can cause losses of human lives, regulatory penalties, damaging recalls of vehicles, damage to the brand, and liabilities for vehicle manufacturers. In this context, the power supply of the safety-relevant applications is of crucial importance since, without it, the respective application cannot be performed [1,2]. Both the literature and practice show that faults in the wiring harness occur across different manufacturers and vehicle segments. It is therefore essential to have a diagnostic that can identify faults in the wiring harness with sufficient reliability using existing automotive measurement systems. The integrity of the safe power supply for the safety-relevant systems is provided by the power feed, the freedom of interference in the powernet, and the power distribution. The power distribution always consists of a wiring harness, which is made up of different components such as cables, connector systems, and splices. A typical wiring harness path for the connection of an electric power steering system is shown in the Figure 1 [3].

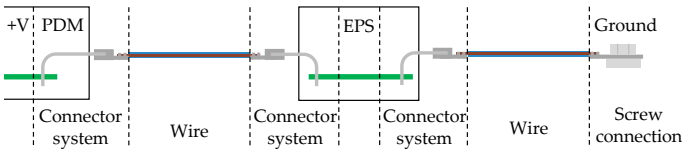


Figure 1. Typical components of a single wiring harness connection of an electric power steering system.

This figure shows that the electric power steering (EPS), as a typical example for a safety-relevant consumer, is connected to a power distribution module (PDM) on the

left-hand side and to the ground on the right-hand side. To ensure power distribution to safety-relevant consumers, either the consumer can be supplied redundantly or a diagnostic must determine that the condition of the wiring harness is in a proper state. Firstly, the functional safety requirements for the wiring harness are discussed. The fault modes of a wiring harness are then examined, whereby an increase in resistance in the components can often be found as a fault in the literature and practice. The diagnostic approach and its implementation are then presented. The approach is then analyzed with the use of simulations, including real measurement deviations, and demonstrated in an experimental study in a vehicle. Finally, the advantages of the approach, additional to achieving functional safety, are highlighted and an outlook is given.

1.1. Safety Requirements for Power Distribution

In the wiring harness, the following three failure modes are relevant and must be considered for safe power distribution [4]. The first failure mode, a short circuit to ground (SCG), is a connection of the positive potential to the ground potential of the vehicle's chassis. This fault is disconnected by a conventional or electrical fuse to protect the wiring harness against overcurrent. An SCG can be prevented by a full taping of the wiring harness and robust routing through the vehicle. The second failure mode, an open circuit (OC), can occur when a connection breaks off. This can be avoided by measures such as strain relief or fault-tolerant connector systems. In summary, SCG and OC failure modes lead to consumers without power supply and occur immediately. This fault is diagnosed due to the corresponding consumer is no longer operational or is not sending any signals.

The third failure mode, a high resistance (HR), results in excessive voltage drop across the wiring harness and, therefore, in a fault or restricted function of the safety-relevant consumers. Hence, an increase in wiring harness resistance must be taken into account in the design, by defining a worst-case voltage drop over the wiring harness path. Over the life cycle, the resistance increases due to environmental influences such as temperature changes and vehicle vibrations, causing the voltage drop to be above the defined worst case before the end of the vehicle's life cycle.

The HR failure mode is critical for load-dynamic safety-relevant consumers, when the resistance of the wiring harness path is so high that nominal currents lead to such an voltage drop. Therefore, an HR failure mode does not have impact during normal operation but causes a high voltage drop at high power demands that might occur in critical situations. For example, an EPS can fail during a power-intensive evasive manoeuvrer due to excessive voltage drop across the wiring harness. Without the new diagnostic approach the resistance increase of the wiring harness will be not diagnosed and hence, is a latent fault. This is particularly relevant for safety-relevant consumers that are only supplied via a single wiring harness path and therefore have no redundancy available.

1.2. Increase of the Wiring Harness Resistance over Lifetime

Figure 1 shows the typical wiring harness path from a power distributor to the EPS and from the EPS to the chassis ground. Every component within this path can increase in their resistance [5].

1.2.1. Environmental Stresses on Components

Every component of the wiring harness is exposed to environmental stresses, leading to different failure modes. The main influences are temperature, corrosive gas attack, vibration, humidity, and moisture [6,7]. Each component reacts in a different way to the environmental stresses.

Connector Systems

As shown in Figure 1, three connector systems are necessary. The interaction of the stresses can lead to a change in the resistance, whereby the resistance of the connector system can increase by a multiple of the initial resistance [8–11]. The most common cause

of resistance increase is due to vibrations and temperature fluctuations, which lead to the wear of the contact surface. This wear leads to oxidation. As a result, at high currents, the connector system can be thermally overloaded and may fail [12,13]. The extent to which connector systems are prone to degradation depends on a number of different factors, such as actual current flow, the material of the contact surface, or tightness against water entry. Therefore, field studies were carried out concerning the failure modes of connector systems. As found from [3], in (maximum) 36-month-old vehicles, about 15 percent of the failures are due to a random cause, such as corrosion. For high-mileage vehicles, field tests by [6,14] have demonstrated a resistance increase of more than three times of the initial resistance. In Laporte [15], the contact resistance is rated as faulty when it has increased by 4 mΩ. Faults in connector systems can lead to extensive recalls [16].

Bolted Connection System

As shown in Figure 1, the EPS is connected to the ground via a screw connection system. Experimental investigations, issues in the field, and [5] suggest that an increase in resistance can occur on screw connection systems. Factors such as a decrease in the connection force due to the loosening of the bolted connection, temperature fluctuations (especially when using different metals), and wear have an influence on the conductivity [17]. A connection system insufficiently bolted to the ground can lead to recalls in the field [18,19].

Electrical Wiring

As shown in Figure 1, two wires are required to connect to the power distribution module and to connect to ground. Their insulation can be damaged by thermal cycling or external damage. This can lead to the SCG or OC failure mode. However, if a wire is used according to its defined specification, no resistance increase is expected [20].

1.2.2. Misapplication or Improper Design

In addition to the degradation of the wiring harness, the resistance may also increase due to misapplication or improper design. These refer, on the one hand, to the different phases of the life cycle, such as manufacture, assembly, or customer operation, and, on the other hand, to correct use, such as compliance with the maximum permissible operating temperature and the minimum bending radius or protection against mechanical damage. If the defined specification and application of each component are not complied to, these can lead to the failure modes SCG, OC, and HR [3,5,21]. To avoid these failure modes, vehicles at risk of an inadequate connection are recalled for inspection [22].

1.3. Novel Diagnostic Approach

Studies have shown that wiring harness resistance can increase over the service life of a vehicle. In the worst-case scenario, this can lead to recalls and, therefore, to enormous costs for car manufacturers. The safety requirements derived from Section 1.1 and studies by [5] led to the conclusion that a reliable diagnostic to identify an increase in resistance contributes to the safe power supply of safety-relevant consumers. This means that there are multiple factors that require a diagnostic to determine the wiring harness resistance.

To match the demand, the diagnostic must fulfill the following three requirements. First, the diagnostic must reliably determine the electrical resistance of the wiring harness path. In this way, the failure mode HR should be detected. Second, the influence of the communication bus and different sample times must be taken into account, if the electrical quantities are measured at different electronic control units (ECUs). Third, measurement errors must be considered in the diagnostic. Thus, for each measurement point, it must be taken into account that it can have an additive and a multiplicative error as well as measurement noise.

In order to exclude an HR failure mode due to an excessive voltage drop across the wiring harness, a resistance must be measured and compared to a resistance limit. For this purpose, for example, a maximum voltage drop $U_{\mathrm{drop}} = 1\,\mathrm{V}$ is defined over

the wiring harness path. This must not be exceeded when the maximum current occurs. In the case of EPS, this can be up to $I_{\text{max,EPS}} = 120\,\text{A}$, which leads to a resistance limit of $R_{\text{limit}} = 8.34\ \text{m}\Omega$ [23,24].

2. Methods

To fulfill the requirements, a novel diagnostic approach to determine the resistance of a wire harness path is presented.

2.1. Physical Derivation

As shown in Figure 2, at least the voltage measuring points U_{PDM} and U_{EPS}, as well as the current measuring point I_{EPS}, are necessary.

$$R_{\text{EPS}} = R_1 + R_2 = \frac{U_{\text{PDM}} - U_{\text{EPS}}}{I_{\text{EPS}}} \tag{1}$$

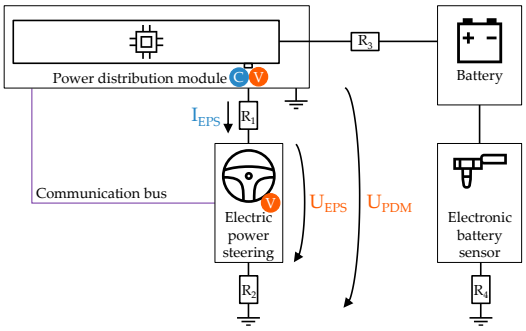


Figure 2. Measurement points in wiring harness topology to determine the wiring harness path resistance.

Measuring points at the power supply (the battery in Figure 2) are not sufficient, as additional resistance (R_3 and r_4) is present due to further wiring harnesses and the current being distributed to several consumers. Therefore, voltage U_{PDM} and current I_{EPS} must be measured at the power distribution module. The power supply, the EPS, and the distributor have separate connections to the chassis ground. However, investigations show that the voltage drop across the chassis itself can be neglected.

In order to fulfill the requirement from Section 1.3, the diagnostic is designed as shown in Figure 3 and the method is explained in the following.

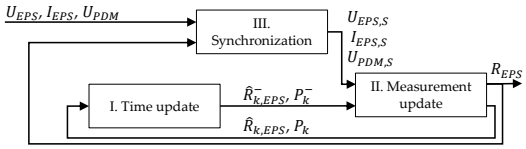


Figure 3. Functional design of the diagnostic.

2.2. Estimation of the Wiring Harness Path Resistance

To estimate the resistance R_{EPS}, an estimator for non-linear systems is necessary to compensate for the influence of the measurement deviation. Various estimation methods, such as least square methods and particle filters, were investigated. The best results were achieved with the extended Kalman filter (EKF). Welch [25] describes the EKF principle design and functionality as well as the nomenclature that will be used from this point on. The EKF estimates a resistance so that the voltage at the EPS is equal to the voltage at the PDM minus the voltage drop across the wiring harness.

$$h(\hat{R}^-_{\text{k,EPS}}, 0) = U_{\text{k,PDM,S}} - I_{\text{k,EPS,S}}\hat{R}^-_{\text{k,EPS}} \tag{2}$$

The task of the EKF is to estimate the resistance in order to predict the voltage at the EPS.

$$z_k = U_{k,EPS,S} \tag{3}$$

Thus, the residual r can be determined, which reflects the deviation between estimated and measured voltage at the EPS.

$$r_k = z_k - h(\hat{R}^-_{k,EPS}, 0) \tag{4}$$

The first part of the EKF is shown in Figure 3 as I. Time update. In the first step, the resistance $\hat{R}^-_{k,EPS}$

$$\hat{R}^-_{k,EPS} = \hat{R}_{k-1,EPS} \tag{5}$$

and the error covariance P^-_k with a constant process noise covariance Q are predicted.

$$P^-_k = P_{k-1} + Q \tag{6}$$

The second part of the EKF is shown in Figure 3 as II. Measurement update. This corrects the estimation by the recent measured values. To achieve this, the Kalman gain K_k is calculated.

$$K_k = \frac{P^-_k H^T_k}{H_k P^-_k H^T_k + G} \tag{7}$$

Using this Kalman gain, it is possible to update the estimate $\hat{R}_{k,EPS}$

$$\hat{R}_{k,EPS} = \hat{R}^-_{k,EPS} + K_k(z_k - h(\hat{R}^-_{k,EPS}, 0)) \tag{8}$$

and the error covariance P_k with the measurement.

$$P_k = (I - K_k H_k) P^-_k \tag{9}$$

Consequently, the resistance $\hat{R}_{k,EPS}$ is used as an estimation of the resistance R_{EPS}. This resistance R_{EPS} is then fed back into III. Synchronization in Figure 3. Thus, the accuracy of the resistance estimation improves with each computation step since it leads to a more accurate synchronization. If the error covariance P_k falls below a value of 0.005, a sufficiently reliable estimation is assumed. If this value is exceeded again, the last estimation of the resistance R_{EPS} is taken into account. This means that the distance between several current pulses is irrelevant and, at the same time, the entire current pulse is used to improve the estimation.

In this way, the first requirement from Section 1.3, the determination of the resistance, can be achieved.

2.3. Synchronization of the Measured Quantities

The measurement signals must be synchronised, otherwise the determined resistance would be incorrectly using the Formula (1). At least one measured variable is transmitted via a communication bus, such as LIN, CAN, or FlexRay. Thereby, a constant signal delay cannot be assumed due to jitter and delay in the communication bus. Therefore, a repeatedly synchronization is mandatory. Since the signal delay is shorter than the sampling time of the communication bus, a synchronization r_{delay} can be introduced. This describes the ratio of the delay of the measurement signal D to the sample time t_s.

$$r_{delay} = \frac{D}{t_s} \tag{10}$$

By estimating the ratio between delay and sample time, the synchronization can be accomplished, which fulfills the second requirement from Section 1.3.

2.4. Estimation of the Epistemic Measurement Errors

However, the estimation of the resistance would be strongly biased by the epistemic measurement errors. Therefore, a repeatedly adapting calibration is necessary to reduce the influence of the measurement errors. The simplified representation of epistemic measurement errors in the following formula contains the multiplicative error a from the true value u and the additive error b, which results in the measured value $\tilde{u}$.

$$\tilde{u} = a\,u + b \tag{11}$$

In addition to determining the resistance of the wiring harness path, the EKF simultaneously determines the ratio r_{error} of the measurement error R_{error} to the measurement signal R_{signal}, which can be traced back to the resistance.

$$r_{\text{error}} = \frac{R_{\text{error}}}{R_{\text{signal}}} \tag{12}$$

The ratio of the resistance error, which is due to a measurement error, is estimated. Reducing the influence of the measurement error on the resistance to be determined. In this way, the third requirement from Section 1.3, measurement errors are considered in the diagnostic.

2.5. Excitation and Optimisation

To determine the resistance, a sufficiently large voltage drop across itself is necessary. This can be provided either by a requested excitation or, in the case of the EPS, by a steering manoeuvrer.

To better compensate measurement errors, the optimization of measurement noise covariance G and process noise covariance Q can be fine-tuned. Furthermore, the resistance R_{EPS} can be estimated accurately faster, depending on the initial parameters $R^{-}_{\text{k}-1,\text{EPS}}$ and $P_{\text{k}-1}$.

3. Results

The presented method is evaluated in the following. Subsequently, the advantages of using the diagnostic are described.

3.1. Simulations

In order to test the proposed diagnostic approach, it was modeled, including the measurement deviation, in the simulation tool MATLAB Simulink Version 18b. The design of the simulation model is according to Figure 2. First, the functionality is examined using a single simulation example. Second, different measurement error combinations are implemented and their influence on the diagnostic result is analyzed.

3.1.1. Single Simulation Example

Figure 4a shows an example input to the diagnostic. The measurement errors and delay shown here are based on the deviations caused by the measurement hardware used in state-of-the-art ECUs and bus systems. Here, an additive error can be observed since the voltage of U_{PDM} and U_{EPS} must be nearly the same if no current I_{EPS} flows. This can occur, for example, due to a ground offset at the voltage measuring points U_{PDM} to U_{EPS}. Since the voltage U_{EPS} is measured at the EPS itself, the measured value must be transmitted to the PDM via a communication bus. IT can be seen in Figure 4 that the edges of U_{EPS} occur slightly delayed after the edges of I_{EPS}.

Figure 4b shows the output of the wiring harness diagnostic (WHD). The determination of the resistance $R_{\text{WHD,EPS}}$ is shown on the top. The true resistance in this simulation model is $R_{\text{true,EPS}} = 6\,\text{m}\Omega$ and the estimated resistance is $R_{\text{WHD,EPS}} = 6.04\,\text{m}\Omega$. Thus, the resistance of the wiring harness path after the current excitation of the EPS could be de-

termined. With this accuracy of resistance determination, the failures shown in Section 1.2 can be recognized. The true delay ratio is $r_{\text{true,delay}} = 25\%$ and the diagnostic estimates this to be $r_{\text{WHD,delay}} = 23\%$. These values indicate that the delay can be determined properly and has only a minor influence on the accuracy of the diagnostic. This means that the measuring points can be distributed across several ECUs. The ratio of the measurement error in the measurement signal is $r_{\text{true,error}} = 46\%$. The diagnostic estimated this ratio as $r_{\text{WHD,error}} = 44\%$. The accuracy of the error determination indicated robustness against measurement errors. This means that the measurement hardware that is already installed in state-of-the-art ECUs can be used. Despite the measurement errors and delay, the diagnostic managed to determine the wiring harness path resistance to the EPS. In this case, the diagnostic was able to ensure that the resistance limit out of Section 1.3 is not exceeded. This means that a failure due to an excessive voltage drop across this path can be excluded and the safety requirement can be fulfilled.

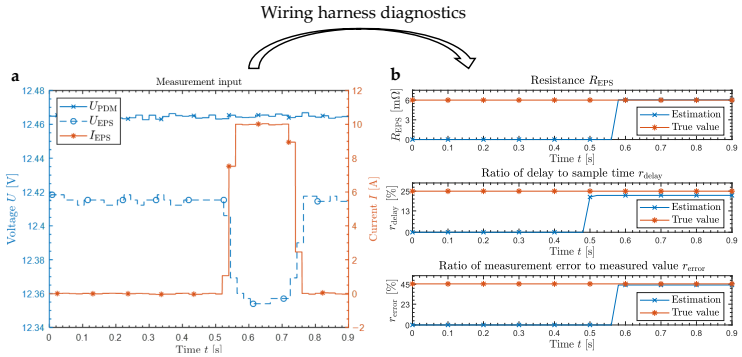


Figure 4. Estimation of wiring harness path resistance R_{EPS}. (**a**) Input with exemplary measurement errors and delay. (**b**) Resistance estimation, delay ratio, and error ratio bias out of the diagnostic.

3.1.2. Validation of the Diagnostic

In order to investigate the behaviour of the diagnostic with different measurement errors, a Monte Carlo experiment is performed. The measurement errors were derived experimentally and from the specifications of a PDM and EPS. In this way, a wide variety of different combined measurement errors can be investigated and thus the diagnostic can be studied in different scenarios. A Monte Carlo simulation offers the advantage that the robustness of the EKF can be analyzed. Furthermore, by repeating simulations, the influence of measurement noise can be better reflected and various possible combinations of measurement errors can be investigated. For this purpose, a uniform distribution of the individual measurement errors of state-of-the-art ECU hardware is used for each measurement point and each time delay, which corresponds to a bus delay via CAN. Using Formula (11), the input $\tilde{u}$ is calculated with the errors from Table 1.

Table 1. Measurement errors for each measurement point and delay.

Error	U_{PDM}	U_{EPS}	I_{EPS}	D
Multiplicative error a	1 ± 0.0375	1 ± 0.021	1 ± 0.0372	0
Additive error b	$\pm 140.1\,\text{mV}$	$\pm 93.6\,\text{mV}$	$\pm 2100\,\text{mA}$	$2.5 \pm 2.4\,\text{ms}$

For each simulation run, random values of a and b are chosen for each error individually according to their uniform distribution.

Figure 5 shows the distribution of R_{EPS} after 1000 simulation runs. The deviation between mean value μ and true value can be attributed to the random selection of the measurement errors. With an increase in the simulation runs, this deviation becomes lower. The variance can be traced back to the measurement errors. In this example, after 1000 runs, a maximum of $\pm 1\,\text{m}\Omega$ is misestimated. This must be taken into account to ensure that the resistance limit in Section 1.3 is not exceeded. Thus, it must be assumed that, if the

resistance was estimated to be above $R_{\mathrm{WHD,limit}} = 7.34\,\mathrm{m\Omega}$, the resistance limit may have been exceeded. If an initial resistance of the wiring harness is known, a resistance change of 4 mΩ, as shown in [15], can also be applied.

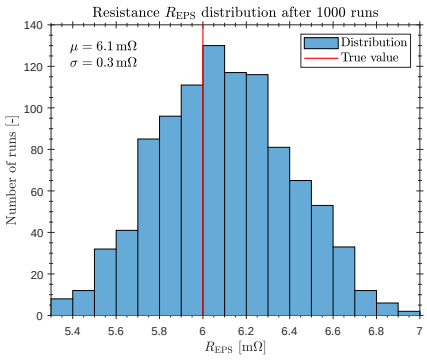


Figure 5. Resulting R_{EPS} after 1000 runs of Monte Carlo simulation. The estimated resistance has a mean value of $\mu = 6.1\,\mathrm{m\Omega}$ and a standard deviation of $\sigma = 0.3\,\mathrm{m\Omega}$.

Figure 6 shows the influence of the multiplicative and additive errors of the different measurement points. The time delay has no relevant influence on the result and is therefore not shown. The additive errors, which are shown in Figure 6a–c, have a little influence on the estimated resistance since these errors are detected by the diagnostic and are included in the error ratio in (12) accordingly.

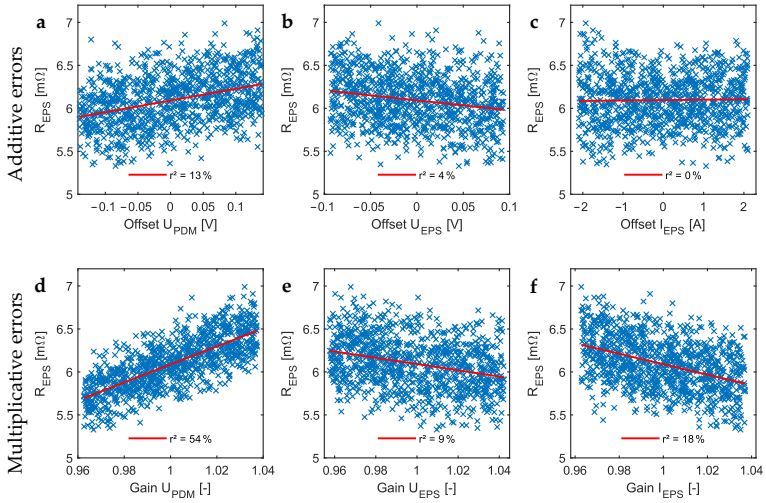


Figure 6. Influence of different measurement errors at all measurement points on resistance estimation.

The multiplicative errors, which are shown in Figure 6d–f, have the main influence on the deviation. Since these measurement errors of the diagnostic appear like a variation of the resistance, these cannot be easily included in the error ratio in (12). Therefore, they have a direct influence on the deviation of the resistance estimation. However, part of the voltage multiplicative error a of U_{PDM} and U_{EPS} can also be reasonably interpreted as an additive error, since the voltage is normally around 12.5 V, making the multiplicative error appear like an additive error. However, a deviation between true and estimated resistance should always be expected since the EKF always assumes a noise in each measurement. The red lines in Figure 6 show the correlation between the estimated resistance and the measurement error determined by simple linear regression. Furthermore, the regression coefficient is shown at the bottom of each plot. Using simple linear regression, 98 percent of the resistance estimation deviation can be attributed. The remaining 2 percent could be attributed to the measurement noise. Additional investigations of the diagnostic showed

that the resistance estimations vary depending on the resistance to be determined and the current excitation.

To further improve the results, each multiplicative error can be additionally estimated by a second measurement point. An additional calibration of the voltage measurement point U_{PDM} would further improve the result. Another possibility would be varying current excitations. The wiring harness resistance changes relatively slowly over its lifetime. Hence, the evaluation of the estimated resistance can be carried out at the end of the driving cycle.

With the measuring points shown in Figure 2, it is not possible to determine which part of the wiring harness has an increased resistance. This would require additional voltage measuring points, which, for example, measure the voltage behind the connector systems in order to monitor individual increases in resistance.

3.1.3. Experimental Validation

In order to investigate the capabilities of the diagnostics in a real environment, it was implemented in a test vehicle. The diagnostics is running on the PDM and the EPS sends the voltage signal to the PDM via CAN.

The measured voltages and current as well as the result of the diagnostics are shown in Figure 7. A steering input when parking has caused the EPS to assist the driver. This caused a power demand and, therefore, a current flow through the wiring harness of the EPS. This resulted in a voltage offset between the PDM and EPS. This was sufficient for the diagnostics to determine the resistance at the end of the current profile. The true resistance was determined before the tests when the vehicle was modified. The cyclical voltage change is due to an alternating set voltage of the DC/DC converter. The values r_{delay} and r_{error} were not included, as these true values in a real test environment are unknown.

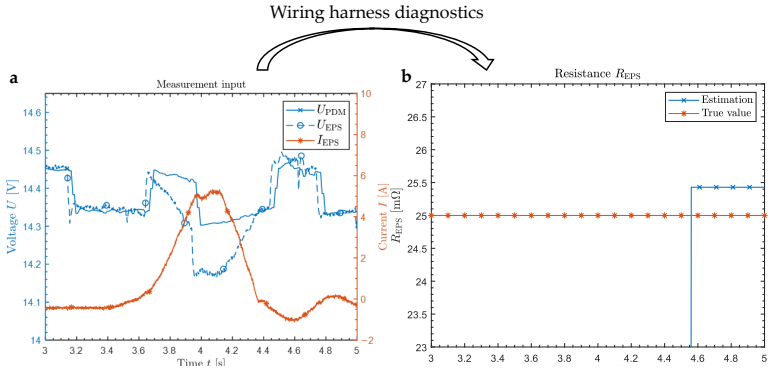


Figure 7. Estimation of EPS wiring harness path resistance R_{EPS} in vehicle. (**a**) Measurement input from PDM and EPS. (**b**) Resistance estimation by using the diagnostic approach.

3.2. Advantages by Using the Diagnostic

In addition to preventing failures due to increased wiring harness resistance, the diagnostic provides further advantages.

3.2.1. Diagnostic Instead of Redundancy

In order to fulfill the safety requirement of the safety-relevant consumers for safe power distribution, either a robust connection or a redundant power supply must be used. However, redundancy is always associated with additional weight and costs as well as more installation space. The diagnostic coverage makes it possible to make redundancy obsolete [4,26].

3.2.2. Design with Less Expensive Materials

In order to increase the robustness of connector systems in the wiring harness, different materials are available for coating. Gold, silver, and tin are the most common materials for coating in connector systems. Silver, for example, is more robust than tin but less than gold

against an increase in resistance [3,7]. Thus, it is possible to use cheaper materials with the help of the diagnostic.

3.2.3. Miniaturization of the Wire Harness Cross-Section

Another advantage can be gained in the design of wiring harnesses. If resistance can be monitored continuously, fewer worst-case assumptions need to be made to guarantee the robustness of the wiring harness over its lifetime. Studies of connector systems used in high-mileage vehicles indicate that only a small proportion of connector systems begin to degrade [6,14]. Laboratory studies also indicate that some connector systems will not increase their resistance [27]. By monitoring the resistance, an increase could be accepted without being safety-critical. Thus, to reduce cost and weight, a smaller cross-section could be used in the design. However, it should be noted that, if the diagnosed wiring harness path degrades, this will be detected by the diagnostic. This makes the fault easy to locate, but a part or the whole path must still be repaired or replaced in a workshop.

3.2.4. Diagnostic of the Entire Power Supply Path

A sensible extension would be to also consider the power supply of the PDM from the battery in Figure 2. Thus, instead of a threshold resistance, the voltage drop over the entire power supply path U_{drop} could be considered, taking into account expected currents I_{EPS} and I_{Batt}. This voltage drop can then be compared against a voltage value.

$$U_{\text{drop}} = R_{\text{EPS}} I_{\text{EPS}} + (R_3 + R_4) I_{\text{Batt}} \tag{13}$$

Therefore, an individual resistance increase of a wiring harness component can be better compensated before a warning is given [28].

4. Conclusions

Potential faults in wiring harnesses in automotive applications were investigated, whereby an increase in resistance can occur at different parts of the wiring harness. As a safety hazard, it was found that an increase in resistance in the wiring harness is only detected when failures of safety-relevant consumers, such as the electronic power steering, occur. Therefore, a diagnostic was developed using a parameter estimation, which estimates the wiring harness resistance using an extended Kalman filter. Different measurement errors and delay were modeled and their influence on the robustness of the diagnostic was investigated. This diagnostic estimates reliably the resistance in milliohm range with a standard deviation of $\sigma = 0.3\,\text{m}\Omega$. The results shown were achieved with the measurement accuracy of state-of-the-art ECUs, meaning that no additional measurement hardware is required. As the delay caused by the bus communication had no relevant influence on the diagnostic accuracy, the measuring points can, therefore, be distributed across several ECUs. The diagnostic shows what is already possible with state-of-the-art measurement systems and, thus, differs from approaches such as [29,30].

By using diagnostics, failure modes, such as high resistance and the creeping off-circuit of the shown components of the wiring harness, can be identified and prevented. This means that an insufficient power supply to safety-relevant loads due to an excessive voltage drop can be identified, thus preventing a safety hazard. In addition, faults can be diagnosed more accurately, making recalls more selective. Furthermore, large-scale recalls can be prevented by only recalling vehicles with faults in the wiring harness. In addition to fulfilling the safety requirements, it is possible to save a redundant wiring harness as well as to reduce the costs and weight of the wiring. In further studies, the added value is to be quantified in more detail, along with the extent to which the shown diagnostic can provide further advantages with other systems, such as energy or power management.

Author Contributions: Conceptualization, L.B., M.L., J.M. and K.P.B.; methodology, L.B., M.L. and J.M.; software, L.B.; validation, L.B.; formal analysis, L.B., M.L. and J.M.; investigation, L.B., M.L. and J.M.; resources, L.B.; data curation, L.B.; writing—original draft preparation, L.B.; writing—review

and editing, L.B.; visualization, L.B.; supervision, M.L., J.M. and K.P.B.; project administration, L.B. All authors have read and agreed to the published version of the manuscript.

Funding: This research received no external funding.

Data Availability Statement: The original contributions presented in the study are included in the article, further inquiries can be directed to the corresponding author.

Conflicts of Interest: Authors Lars Braun, Minh Le and Jürgen Motz were employed by the company Robert Bosch GmbH. The authors declare that the research was conducted in the absence of any commercial or financial relationships that could be construed as a potential conflict of interest.

Notations

The following notations are used in this manuscript.

Symbol	Unit	Description
U_{drop}	V	Voltage drop across the wiring harness of the EPS.
$I_{\text{max,EPS}}$	A	Assumed maximum current of the EPS
R_{limit}	Ω	Resistance limit above which the voltage drop is above the defined voltage drop U_{drop}
R_{EPS}	Ω	Electrical resistance of the wiring harness between PDM, EPS and ground
U_{PDM}	V	Voltage between PDM and ground.
U_{EPS}	V	Voltage at the clamps of EPS
I_{EPS}	A	Current flow through the path of the EPS/Current demand of the EPS
$_{\text{S}}$	-	Notation, indicates that the measured value is time-synchronized
$_{\text{k}}$	-	Indicates the current discrete point in time
$_{\text{k}-1}$	-	Indicates the previous discrete point in time
$\hat{R}^{-}_{\text{k,EPS}}$	Ω	The a priori estimated resistance of the wiring harness at the discrete point in time $_{\text{k}}$; hat$\hat{}$indicates that this is an estimation; super minus $^{-}$ indicates that this was estimated a priori at the current point in time $_{\text{k}}$
h	V	The function used to calculate the voltage at the steering system using a voltage divide
z	V	The function that returns the measured voltage at the EPS to compare it with the result of the estimation
r	V	Deviation between estimated and measured voltage at the EPS
P	V^2	Error covariance, which represents the measurement deviations, such as noise, and thus has less influence on the estimated resistance
Q	V^2	Constant process noise covariance, which takes into account the offset of the measurements; is pre-calculated using parameter optimization
G	V^2	Constant measurement noise covariance, which takes into account the normally distributed measurement noise; is pre-calculated using parameter optimization
H	A	Jacobian matrix of partial derivatives of h with respect to $\hat{R}_{\text{EPS}}$. In this case, $H = -I_{\text{EPS}}$
K	$\frac{1}{\text{A}}$	The Kalman gain is a factor that defines the influence of the residual r on the estimation
I	-	Identity matrix
D	s	Delay of the measurement signals against each other
t_{EPS}	s	Sample time, which is defined by the periodic transmission of the signal via the communication bus
r_{delay}	%	This describes the ratio of the delay of the measurement signal D to the sample time t_{s}
R_{error}	-	Includes the measurement deviation of the measuring points U_{PDM}, U_{EPS}, and I_{EPS}. Theoretical information.
R_{signal}	-	Contains the true measured values without errors; theoretical information.
r_{error}	%	Ratio of the resistance error, which is due to the measurement error

Abbreviations

The following abbreviations are used in this manuscript:

EPS	Electric Power Steering
PDM	Power Distribution Module
SCG	Short Circuit to Ground
OC	Open Circuit
HR	High Resistance
ECU	Electronic Control Unit
EKF	Extended Kalman Filter
LIN	Local Interconnect Network
CAN	Controller Area Network

References

1. Kilian, P.; Köhler, A.; van Bergen, P.; Gebauer, C.; Pfeufer, B.; Koller, O.; Bertsche, B. Principle Guidelines for Safe Power Supply Systems Development. *IEEE Access* **2021**, *9*, 107751–107766. [CrossRef]
2. Jagfeld, S.M.P.; Weldle, R.; Knorr, R.; Fill, A.; Birke, K.P. *What Is Going on Within the Automotive PowerNet*? SAE Technical Paper, 2024-01-2985; SAE: Warrendale, PA, USA, 2024.
3. Böhm, A. *Ausfallraten für Bordnetz-Komponenten im Automobil—Erwartungswerte und Bedingungen*; ZVEI e.V.: Köln, Germany, 2021. Available online: https://www.bayern-innovativ.de/services/asset/pdf-dokumente/cluster-automotive/zvei-bi-tlf-ausfallraten-bordnetzkomponenten-ausgabe1-oktober2021.pdf (accessed on 12 April 2022).
4. Kilian, P.; van Bergen, P.; Koller, O.; Dazer, M. *Safe Power Supply for a Single-Channel Connected Consumer*; Unpublished Paper; Robert Bosch GmbH: Gerlingen, Germany, 2022.
5. Riera, A. Securisation du reseau de bord 12 V des vehicules autonomes. In Proceedings of the Congrès Lambda Mu 21, HAL, Reims, France, 16–18 October 2018.
6. Swingler, J.; McBride, J.W.; Maul, C. Degradation of road tested automotive connectors. In Proceedings of the 45th IEEE Holm Conference on Electrical Contacts, Pittsburgh, PA, USA, 4–6 October 1999.
7. Bierwirth, F.; Fröschl, J.; Gebert, J.; Herzog, H.G. System Analysis of Vehicle Low-Voltage Energy Paths as Initial Step for a Predictive Diagnosis. In Proceedings of the 15th International Conference on Ecological Vehicles and Renewable Energies, Monte-Carlo, Monaco, 10 September 2020; pp. 1–6.
8. Abdi, R.E.; Carvou, E.; Benjemâa, N. Electrical resistance change of automotive connectors submitted to vibrations and temperature. In Proceedings of the 2015 IEEE Energy Conversion Congress and Exposition (ECCE), Montreal, QC, Canada, 20–24 September 2015; pp. 1910–1913.
9. Bierwirth, F.; Fröschl, J.; Gebert, J.; Herzog, H.-G. Determining Vehicle Energy Paths' Remaining Useful Life using Design of Experiments. In Proceedings of the 15th International Conference on Ecological Vehicles and Renewable Energies (EVER), Monte-Carlo, Monaco, 10–12 September 2020; pp. 1–7.
10. Lee, A.; Mamrick, M. Fretting corrosion of Tin-plated copper alloy. *IEEE Trans. Components Hybrids Manuf. Technol.* **1987**, *10*, 63–67. [CrossRef]
11. Kloch, K.T.; Kozak, P.; Mlyniec, A. A review and perspectives on predicting the performance and durability of electrical contacts in automotive applications. *Eng. Fail. Anal.* **2021**, *121*, 105143. [CrossRef]
12. Schmucker, C.; Meyer, R. Energiebordnetze. In *Batterien, Bordnetze und Vernetzung*; Reif, K., Ed.; Vieweg+Teubner: Wiesbaden, Germany, 2010; pp. 10–35.
13. Fu, R.; Choe, S.-Y.; Jackson, R.L.; Flowers, G.T.; Bozack, M.J.; Zhong, L.; Kim, D. Vibration-Induced Changes in the Contact Resistance of High Power Electrical Connectors for Hybrid Vehicles. *IEEE Trans. Components Packag. Manuf. Technol.* **2012**, *2*, 185–193. [CrossRef]
14. Sawada, S.; Shimizu, A.; Saitoh, Y. Deterioration Analysis of Automotive Connectors Used in High Mileage Vehicles. *SEI Tech. Rev.* **2015**, *81*, 10–15.
15. Laporte, J.; Perrinet, O.; Fouvry, S. Prediction of the electrical contact resistance endurance of silver-plated coatings subject to fretting wear, using a friction energy density approach. *Wear* **2014**, *330–331*, 170–181. [CrossRef]
16. Krok, A. Nissan Recalls Another 125,000 Rogue SUVs for Wiring Harness Issue. Available online: https://www.cnet.com/roadshow/news/nissan-rogue-suv-recall-expansion-wiring-harness-corrosion/ (accessed on 11 July 2024).
17. Braunović, M. Power Connections. In *Electrical Contacts*; Slade, P., Ed.; Marcel Dekker: New York, NY, USA, 1999; pp. 155–278.
18. BBC. Daimler Recalls 400,000 Mercedes-Benz Cars in the UK. Available online: https://www.bbc.com/news/business-41633941 (accessed on 11 July 2024).
19. Fitzgerald, J. Mercedes-Benz Recalls SUVs for Electrical Problem That Could Lead to Fire. Available online: https://www.caranddriver.com/news/a60257844/mercedes-benz-48-volt-grounding-recall/ (accessed on 11 July 2024).
20. *MIL HDBK 217 F*; Military Handbook: Reliability Prediction of Electronic Equipment. U.S. Department of Defense: Washington, DC, USA, 1995.

21. Liu, D.R.; Brackett, T.; Nicastri, P. *Low/High Time-In-Service Behavior of Falsely Locked Automotive Electrical Connector as Demonstrated in a Bench Test*; SAE Technical Papers; SAE: Detroit, MI, USA, 2005.
22. Panait, M. Kia Recalls 2024 Sorento for Incorrectly Assembled Power Steering Wiring Harness. Available online: https://www.autoevolution.com/news/kia-recalls-2024-sorento-for-incorrectly-assembled-power-steering-wiring-harness-232911.html (accessed on 11 July 2024).
23. Kohler, T.P. *Prädiktives Leistungsmanagement in Fahrzeugbordnetzen*; Springer Vieweg: Wiesbaden, Germany, 2014.
24. Pfeffer, P.; Harrer, M. *Lenkungshandbuch*, 2nd ed.; Springer Fachmedien: Wiesbaden, Germany, 2013; pp. 347–408.
25. Welch, G.; Bishop, G. An introduction to the kalman filter. In Proceedings of the SIGGRAPH Course 8, Los Angeles, CA, USA, 12–17 August 2001.
26. Bierwirth, F.; Fröschl, J.; Gebert, J.; Herzog, H.-G. Determining the Diagnosis Corridor for Monitoring Contact Degradations along Vehicle Energy Paths. In Proceedings of the 14th International Conference on Diagnostics in Electrical Engineering (Diagnostika), Pilsen, Czech Republic, 1–4 September 2020; pp. 1–6.
27. Swingler, J.; McBride, J.W. Fretting corrosion and the reliability of multicontact connector terminals. *IEEE Trans. Components Packag. Technol.* **2002**, *25*, 670–676. [CrossRef]
28. Braun, L. Global powernet diagnostics: Miniaturization of the Powernet by using a diagnostic function. In Proceedings of the 9th Bordnetze im Automobil, online event, 12–13 October 2021.
29. Bierwirth, F.; Fröschl, J.; Gebert, J.; Herzog, H.-G. Statistical Method for Health Monitoring of Power Supply Paths in Vehicles. In Proceedings of the 2020 International Conference on Diagnostics in Electrical Engineering (Diagnostika), Pilsen, Czech Republic, 1–4 September 2020; pp. 1–6.
30. Bierwirth, F.; Grottenthaler, Y.; Tippe, L.; Taube, J.; Gebert, J.F.; Herzog, H.-G. Predictive Diagnosis of E-Fuse-Protected Supply Paths in Vehicle Low-Voltage Energy Systems. In Proceedings of the International Conference on Electric and Electronic Systems in Hybrid and Electric Vehicles and Electrical Energy Management (EEHE), Essen, Germany, 8–9 November 2021.

Disclaimer/Publisher's Note: The statements, opinions and data contained in all publications are solely those of the individual author(s) and contributor(s) and not of MDPI and/or the editor(s). MDPI and/or the editor(s) disclaim responsibility for any injury to people or property resulting from any ideas, methods, instructions or products referred to in the content.